Indian Journal of Fibre & Textile Research
Vol. 44, September 2019, pp. 279-285

Spirograph based electrospinning system for producing fibre mat with near uniform mechanical property

P Pathalamuthu[1,a], A Siddharthan[2] & V R Giridev[3]

[1]Department of Chemical Engineering, [2]Department of Production Technology,
[3] Department of Textile Technology, Anna University, Chennai 600 025, India

Received 23 January 2018; revised received and accepted 14 May 2018

This study focuses on the development of Spirograph-based mechanical system (SBMS) for the collection of polyacrylonitrile fibres in an electrospinning process. The collector plate is set to trace a spiropath in such a way that the event of crossing the centre of collection region from different radial direction is high. To assess the capability of SBMS, electrospun mat of acrylic has been prepared and the properties of samples sectioned from different angular positions of a circular mat are evaluated. The diameter and alignment of fibres are analyzed by processing the scanning electron microscopy (SEM) images of electrospun mats with the use of ImageJ software. The electrospun mat produced using SBMS collector assembly exhibits near uniform characteristics like thickness, tensile strength, porosity, fibre diameter and fibre alignment as compared to the electrospun mat produced by using conventional static collector.

Keywords: Electrospun mat, Isotropic property, Mechanical property, Porosity, Polyacrylonitrile, Spirograph

1 Introduction

Typical path of tool head or work piece in the most of manufacturing processes involve regular geometry, like linear, circular, cylindrical profile, etc to achieve the desired shape in surface grinding, turning in a lathe, milling process and mixing by a stirrer. Such processes yield products which have varying characteristic and property from location to location. This may be due to the difference in materials microstructure, tool - material interaction such as texture, roughness, hardness, etc. To minimize the heterogeneity in the characteristics and properties of the product, randomized path of tool- work piece interaction during material processing was commonly implemented. Such randomization is expected to yield uniform properties and characteristics throughout the product at various locations.

However, the use of hypotrocoidal and epitrocoidal path of tool-material interaction were investigated in specific processes like planarization of silicon wafer[1] and stirrer[2] and found to have improved the uniformity in the properties. Besides achieving the uniformity, these kinds of hypotrocoidal and epitrocoidal tool material interaction pathways had enhanced the efficiency of the process[3].

[a] Corresponding author.
E mail: muthup2001in@yahoo.co.in

Electrospinning process is a broadly used technology for nanofibre production with fibre diameter ranging from 2 nm to several micrometers. The electrospun mat is used in wide variety of applications like filter, membrane, scaffold for tissue engineering, wound dressing material and sensor. Electrospinning system consists of three major components, namely a high voltage power supply, a spinneret and a grounded collecting plate. This process involves regulated discharge of polymer solution through a syringe pump. High voltage between syringe and collector causes Taylor cone conversion into stream of jets which gets deposited randomly on a grounded collector due to the bending instability of the highly charged jet[4,5]. Generally, a stationary aluminium foil is used in the laboratory scale production of electrospun mat. Other variants of collectors, such as rotating cylinder, rotating wheel[6-8], wire mesh[9], pin[10] and parallel or gridded bar[11] are used to produce unidirectional and bidirectional aligned nanofibres. The pattern of fibre alignment is determined by the geometrical features of the collector and its speed of rotation[12]. Unidirectional aligned nanofibres is desired in applications like solar cells, fuel cells[13-16], biomedical engineering[17], scaffold for regeneration of nerve & muscle cells[18-20] and chemical & biological sensors[21]. Numerous modifications in the collector plate have been made for producing fibre mat with desired alignment[22-29]. The goal is to improve the

mechanical property of electrospun mat for application such as wound scaffold[30-32] and filtration[33]. The porosity of electrospun mat also plays a vital role in various applications like tissue engineering[34] and wound scaffold. To analyse the uniformity of the properties of electrospun mat, mechanical properties of mat were analysed in different locations at various angles[35]. The distributions of electrospun nanofibre diameters[36] were reported. The diameter and alignment of nanofibres in the electrospun mat were analyzed by using FFT (Image J)[37-39] and by Radon Transform method (MAT LAB)[40].

Spirograph is a geometric drawing tool that produces variety of mathematical roulette curves known as hypotrocoids and epitrocoids. This study aims at developing Spirograph-based mechanical system (SBMS) of collector assembly for an electrospinning process, based on which Indian patent has been filed[41]. The properties of electrospun mat produced using SBMS collector assembly is also compared to the mat prepared by using the conventional stationary collector plate.

2 Materials and Methods

A collector plate in an electrospinning process is either stationary or rotated in fixed axis. The collector plate assembly based on spirograph is designed and named as Spirograph-based mechanical system (SBMS). It is set to move in specific roulette curves during the collection of fibres. Spirograph drawing tool involves meshing of gears. The gear in larger diameter is called outer gear, which has gear tooth along the inner circumference and is kept stationary. The smaller diameter gear is referred as inner gear that revolves by meshing with the outer gear. There are various holes in inner gear for locating the drawing pen.

For the fabrication of SBMS, the location of holes for drawing pen, the ratio between the number of teeth of meshing gears (inner and outer gear) and the diameter of gears of a spirograph drawing tool are scaled to dimensions suitable for the existing electrospinning set up in the laboratory. In SBMS system, the inner gear is rotated using a connector that links centre of the inner gear at one end and motor shaft at the other end. The location, where the drawing pen is placed in case of spirograph drawing tool kit, is the point where the circular collector plate is affixed and referred as the pointer. The location for pointer is selected in such a way that the event of roulette curve crossing the centre from all the directions is maximum. The different positions of pointer in inner gear are illustrated in Fig. 1(a). The detail of outer gear is shown in Fig. 1(b). Various spirograph designs produced by different pointers are represented in Fig. 1(c). The dimension of the connector is depicted in Fig. 1(d). Though different spirograph designs can be generated by fixing the collector plate to the different pointers, pointer location 1 was chosen in this study for the developed SBMS collector assembly. The connector was powered by an electrical motor and a regulator to vary the speed of revolution. Carbon brushes were used to connect the negative charge to the collector plate.

Polyacrylonitrile (PAN) was dissolved in dimethyl-formamide (DMF) for electrospinning process. PAN of 12 wt. % was dissolved in DMF under constant magnetic stirrer in 12-14 h. Electrospinning was carried for 2 h to fabricate mat for all experiments. For comparison, electrospun mat was also fabricated using static collector for the same electrospinning parameters. The size of the collectors in both static and dynamic was 150 mm diameter. The syringe tip to collector distance was fixed at 150 mm. The thickness of the electrospun mat was measured at different locations within different angular sections by using micrometer of least count 0.01 mm. The average of 5 readings per sample was reported.

To analyze the influence of rotation speed of collector plate of SBMS, electrospun mat was prepared at various speeds, namely 200, 300 and 400 rpm. The morphology of the fibre mat produced by conventional static collector assembly and SBMS setup were studied by using SEM (TESCAN VEGA3 SBU, USA). A small section of fibre mat was mounted onto the SEM sample holder using conductive black carbon tape and gold sputtered prior to analysis.

The porosity of the eletrospun nanofibre mat was measured using a capillary flow porometer (Porous Materials Inc., USA). A wetting liquid Galwick$_{TM}$ (Porous Materials Inc., USA) was applied to fill the pores in the electrospun mat at differential pressures of nitrogen. The supply of gas was slowly increased to the sample so as to remove the liquid filling the pores and entrain gas flow. The differential pressure and flow rates through dry and wet electrospun mats were used for determination of porosity, as shown below:

$$D = \frac{4\,\lambda Cos\,\theta}{P}$$

where D is the pore diameter; λ the surface tension of the wetting liquid; Θ, the contact angle of the wetting liquid; and P, the differential pressure

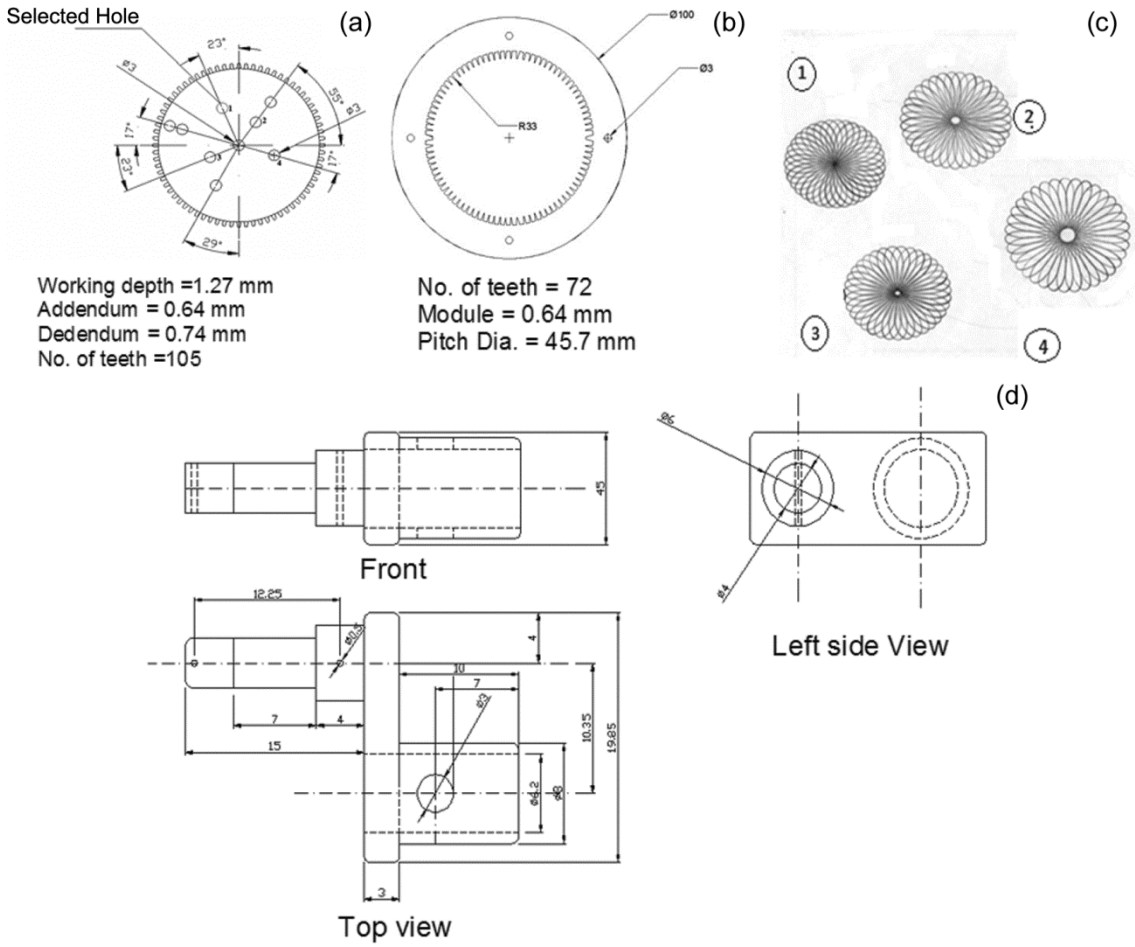

Fig. 1 — Fabrication of SBMS (a) inner gear, (b) outer gear, (c) spirograph designs, and (d) connector (all dimensions are in mm)

The diameters and alignment of the fibres were characterised by using NIH (National Institutes of Health) imageJ software. DiameterJ was a plugin used in imageJ (Fiji) software to analyze the diameter of nanofibres on electrospun SEM images. FFT method was used to evaluate relative fibre alignment in electrospun mat.

To section mat of uniform size as per ASTM standard D882 at different angular location (0˚, 30˚, 60˚, 90˚ …), a template made out of card board was used. Specimens of size 20 mm × 10 mm was sectioned from the electrospun mat produced using both static and SBMS collectors. The specimens were tested by using a Universal Testing Machine (UTM, Instron 3369). The cross head speed for the tensile test was 5 mm/min. The results represented the average of 5 samples.

3 Results and Discussion

The graph between thicknesses of the mat was produced by using SBMS collectors operated at various rpm and different angular sections of the electrospun mat (Fig. 2). It indicates that the mat produced by using SBMS collector has uniform thickness than one produced by using static collectors. It is because the SBMS collector rotates multi directionally defined spirographic path. In the static collector, the fibre deposition initially takes on the place which has more conductivity and then moves to other place. So, the fibres are deposited in different place in static collector. Generally, mat with uniform thickness throughout the electrospun is expected to have uniform mechanical properties.

The mat produced using SBMS collector operated at 300 rpm and 200 rpm has nearly uniform thickness with less variations. The distribution of pore sizes of the electrospun mat produced at different rpm of collector was in the range of 0.1 - 39 μm. The electrospun mat produced using SBMS collector assembly shows narrow distribution of pore size than that of mat produced using static collector [Figs 3 (a) and (b)]. The distribution of pore size of electrospun

mat produced using SBMS collector operated at 300 rpm has uniform porosity. The higher rotational speed of the collector omitted the deposition of nanofibres due to the air flow in the surface of the collector.

It is observed that the fibres are deposited throughout the collector plate using the SBMS collector unlike static collector, which shows uneven deposition (Fig. 4). In SBMS collector system, the

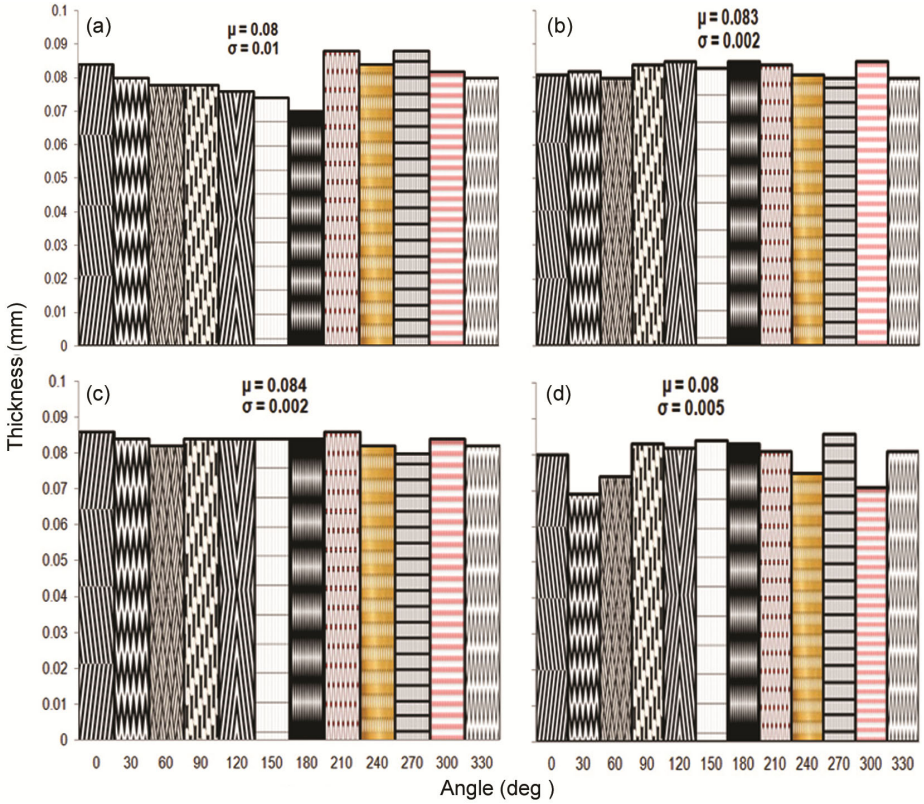

Fig. 2 — Variation in thickness at various angular sections of electrospun mat produced using static collector (a), and SBMS collector operated at 200 rpm (b), 300 rpm (c), and 400 rpm (d) [μ- Average and σ- Standard Deviation from mean]

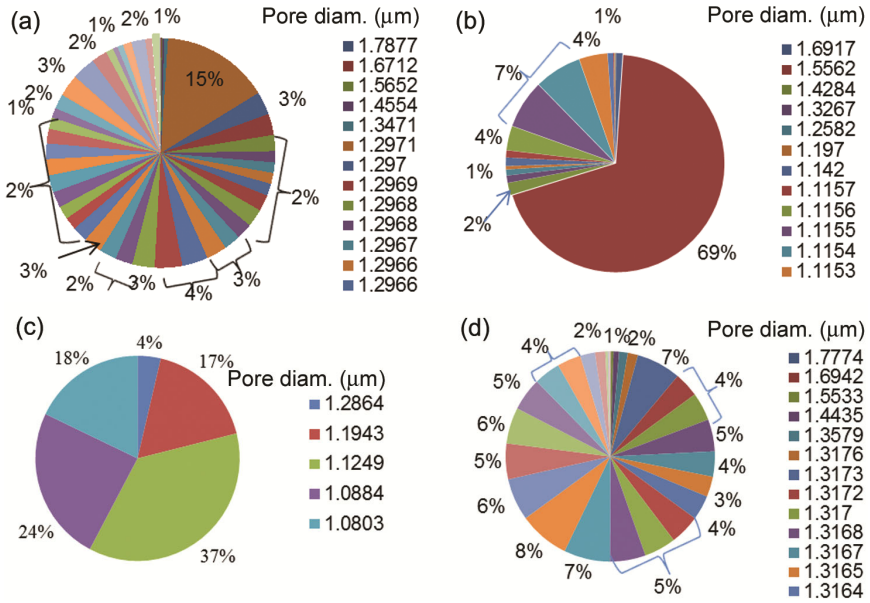

Fig. 3 — Porosity analyses of mat prepared using static (a), and SBMS collector operated at 200 rpm (b), 300 rpm (c) , and 400 rpm (d)

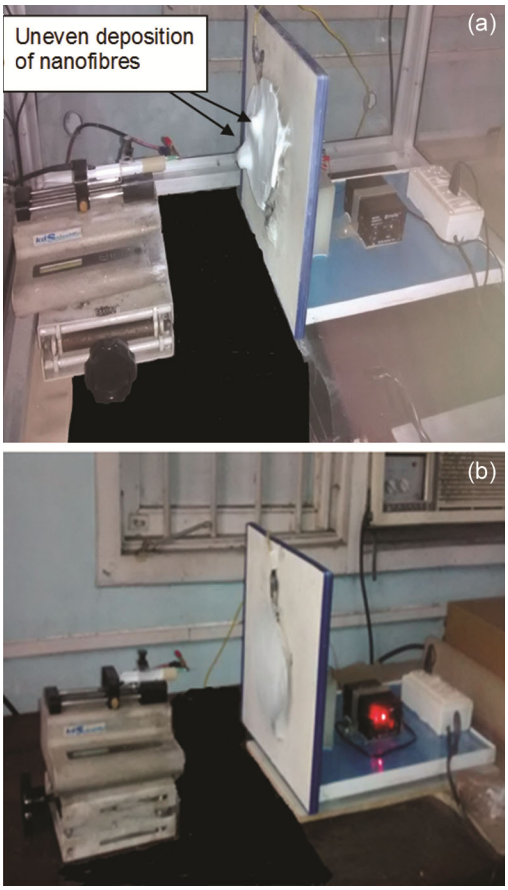

Fig. 4 — Comparison of static and SBMS collector intermittently during the collection (a) static collector and (b) SBMS collector

nanofibres are deposited uniformly throughout entire collector plate due to the nature of movement of collector plate.

Figure 5 describes that the deviation of tensile strength, Young's modulus of sectioned mat are at different angular sections. The trend depicted that the variation among the various sections of the electrospun mat is least for the rotating speed of 300 rpm using SBMS collector. The rotating collector and induced air flow interact with the stream of jet. The force of interaction increases with rotation speed of collector plate. So, the increasing rotational speed of the collector plate leads to uneven deposition of fibres. Fracturing of the fibres occurs due to very high rotating speed of the collector[42]. Mechanical properties of electrospun scaffold are mainly influenced by alignment of the fibres[43,44]. The well aligned nanofibres show improved mechanical property when compared to randomly deposited nanofibres[45].

The trend shows that for speed greater than 300 rpm, the mechanical property decreases[46]. From

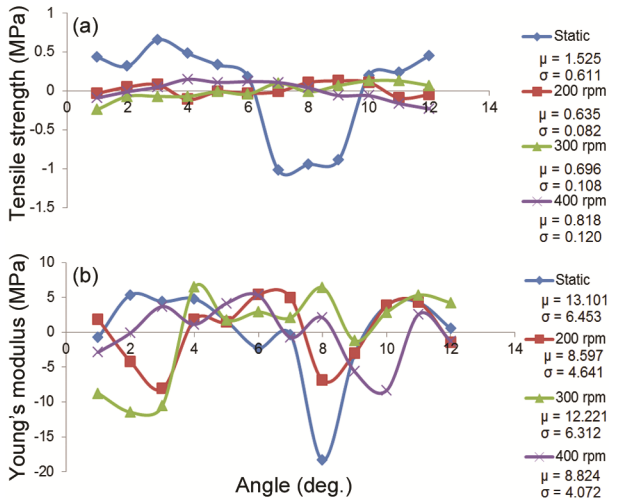

Fig. 5 — Property (deviation from mean) of electrospun mat sectioned from different angular regions from the overall average value (a) tensile strength and (b) Young's modulus

the analysis of electrospun mat produced at various rpm, 300 rpm is chosen for further analysis. Hence, SBMS collector operated at 300 rpm is selected for further comparative study with conventional static collector. The SEM morphology of the electrospun mat shows nano dimension of fibres. The SEM images of electrospun mat produced by using static and SBMS collector are depicted in Fig. 6.

The FFT analysis results are shown in Fig. 6. Overall observation of 2D –FFT analysis shows that the alignment of fibres almost has uniform distribution of fibres in the mat produced by using SBMS collector than that of static collector.

At the onset of electrospinning process, the fibres are deposited at concentrated locations and they are favourably conductive. Once the conductive path in that region gets reduced with fibre deposition, the deposition starts at other regions. But in the case of SBMS, the fibres deposition is based on the conductive path, movement of collector path in spirograph pattern and also due to the interaction of jet and air flow induced by rotating collector plate. The diameter of the nanofibres and orientation of the fibres in the SEM image are analyzed by ImageJ software. Figure 6 give the detailed diameter analysis process performed by ImageJ. From the diameter analysis, porosity and number of fibre intersection are observed as depicted in Table 1. The average fibre diameters are 748 nm and 593 nm in static and SBMS respectively. The fibre diameter variation is more in mat collected using static collector as compared to SBMS collector. In the static collector, the deposition

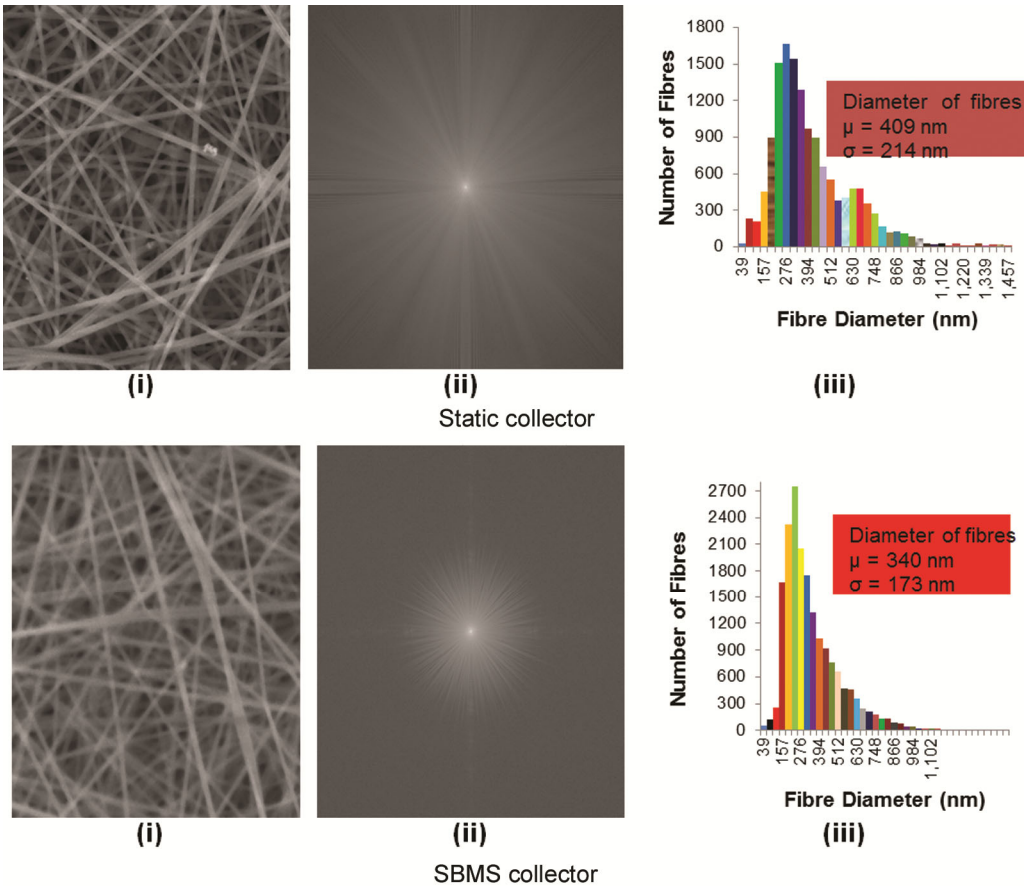

Fig. 6 — FFT analysis of electrospun mat produced (i) SEM image of scaffold, (ii) 2D FFT analysis and (iii) diameter analysis

Table 1— Porosity analysis of electrospun mat through diameter

Property	Static	SBMS
Mean pore area, μm^2	1.62	1.062
Minimum pore area, μm^2	0.042	0.013
Maximum pore area, μm^2	10.25	10.21
Number of pores	100	173
Number of intersections	290	447

of fibres is more when the conductivity is more. The deposition of nanofibre is moved to other place after decreasing the conductivity. So, the continuous deposition of fibres at one particular place increases the fibre diameter and more variations in the diameter range.

The diameter analysis of mat produced using the static collector shows fibres in the range of 39 -1457 nm. But the mat produced using SBMS has diameter in the range of 39-1220 nm. So, the variations in diameter of the nanofibres are very less in SBMS mode. The mat produced using SBMS describes more number of intersection points (fusion) as compared to mat produced by using static collector. If the number of fusion points in the electrospun mat is more, the mechanical property of the mat[47], will increase. The alignment of the fibres in the electrospun mat can be further improved by using magnetic fields and electrodes[48, 49].

4 Conclusion

The developed SBMS collector produces mat with more number of fusion points, more or less uniform thickness, improved fibre orientation, mechanical property and porosity than that of electrospun mat produced by using static collector. The nanofibre diameter decreases in SBMS as compared to that in static collector. The rotational speed of collector plate of SBMS influences the deposition of fibre and 300 rpm is found to be the optimal in the present investigation. The developed SBMS can be further improved by selection of different roulette curves. The uniform property of mat produced by using SBMS may be promising and productive for usage in healthcare and filter applications.

References

1 Pietsch G J & Kerstan M, *Precis Eng*, 29 (2005)189.
2 Sousa F J P, Hosse D S, Reichenbach I, Aurich J C & Seewig J, *J Mater Process Technol*, 213 (2013) 728.
3 Tsuyoshi K & Saki U, *Topology Appl*, 157 (2010) 280.
4 Reneker D H, Yarin A L, Fong H & Koombhongse S, *J Appl Phys*, 87(9) (2000) 4531.
5 Shin Y M, Hohmanm M M, Brenner M P & Rutledge G C, *Appl Phys Lett*, 78 (8) (2001) 4721.
6 Mi H Y, Jing X, Yu E, Wang X, Li Q & Turng L S, *J Mech Behav Biomed Mater*, 78(2018) 433.
7 Cai J, Liu X, Zhao Y & Guo F, *Desalination*, 429(2018**)** 70.
8 Tonya J W, Christian Oliver C A & Harini G S, *J Biomed Mater Res*, 16A (1) (2018) 1.
9 Wang Y, Wang G, Chen L, Li H, Yin T, Wang B, Lee, J C M & Yu Q, *Biofabrication*, 1(1) (2009) 1.
10 Sundaray B, Subramanian V & Natarajan T S, *Appl Phys Lett*, 84(7) (2004) 1222.
11 Li D, Wang Y & Xia Y, *Adv Mater*, 16(4) (2004) 361.
12 Kumbar S G, James R, Nukavarapu S P & Laurencin C T, *Biomed Mater*, 3(2008) 1.
13 Shim H S, Kim J W & Kim W B, *J Nanosci Nanotechnol*, 9(2009) 4721.
14 Liao I C, Chew S Y & Leong K W, *Nanomedicine (Lond)*, 1(2006) 465.
15 Tamura T & Kawakami H, *Nano Lett*, 10(2010) 1324.
16 Dissanayake M A K L, Sarangika, H N M, Senadeera G K R, Divarathna, H K D W M N R & Ekanayake E M P C, *J Appl Electrochem*, 47(2017) 1239.
17 Meng Z X, Wang Y S, Ma C, Zheng W, Li L & Zheng Y F, *Mater Sci Eng C*, 30(2010) 1204.
18 Theron A, Zussman E & Yarin A L, *Nanotechnology*, 12(2001) 384.
19 Bhattarai N, Edmondson D, Veish O, Masten F A & Zhang M, *Biomaterials*, 26(2005) 6176.
20 Cooper A, Jana S, Bhattarai N & Zhang M, *J Mater Chem*, 20(2010) 8904.
21 Zhang M, Zhao X, Wei G & Su Z, *J Mater Chem B*, 5(2017) 1966.
22 Sundaray B, Subramanian V, Natarajan T S, Xiang R Z, Chang C C & Fann W S, *Appl Phys Lett*, 84(2004) 1222.
23 Katta P, Alessandro M, Ramsier R D & Chase G G, *Nano Letters*, 4(2004) 2215.
24 Chuangchote S & Supaphol P, *J Nanosci Nanotechnol*, 6(2006) 125.
25 Khamforoush M & Mahjob M, *Materials Letters*, 65(2011) 453.
26 Park S H & Yang D Y, *J Appl Polym Sci*, 120(2011) 1800.
27 Afifi A M, Yamamoto M, Yamane H, Kimura Y, Salmawy A E & Nakano S, *J Soc Fiber Sci Technol Jpn*, 67(2011**)** 103.
28 Mincheva R, Manolova N & Rashkov I, *Eur Polym J*, 43(2007) 2809.
29 Sahay R, Thavasi V & Ramakrishna S, *J Nanomater,* 2011(2011) 1.
30 Farboodmanesh S, Chen J, Pelealuw J L & Cloutier D E, *NSTI-Nanitech*, 2(2008) 1.
31 Hussain M M & Ramkumar S S, *Indian J Fibre Text Res,* 31(2006) 41.
32 Tarun K & Gobi N, *Indian J Fibre Text Res,* 37 (2012) 127.
33 Huang L & McCutcheon, J R, *J Memb Sci*, 457(2014) 162.
34 Vaquette C, John J & White C, *Acta Biomater*, 7(2011) 2544.
35 Robert L M, Brendon M B, Nandan L N, Jason A B, Wan-Ju li, Rocky S T & Dawn M E, *Tissue Eng Part B Rev*, 15 (2) (2009) 171.
36 Malasauskiene J, Milasius R & Kuchanauskaite E, *Fibers Text East Eur*, 2(116) (2016), 23.
37 Ayres C E, Shekhar Jha B, Meredith H, Bowman J R, Bowlin G L, Henderson S C & Simpson D G, *J Biomater Sci Polym Ed*, 19(5) (2008) 603.
38 Wang H B, Mullins M E, Cregg J M, McCarthy C W & Gilbert R J, *Acta Biomater*, 6(2010) 2970.
39 Abualrejal M M A, Zou H, Chen J, Song Y & Seng Y, *Advances in Nanoparticles*, 6(2017) 33.
40 Schaub N J, Gilbert R J & Kirkpatrick S J, *Proc. SPIE* , 7897(2011) 1.
41 Pathalamuthu P, Siddharthan A & Giridev V R, *Indian Pat 5603, 2014.*
42 Edwards M D, Mitchell G R., Mohan S D & Olley R H, *Eur Polym J*, 46 (6) (2010) 1175.
43 Mauck R L, Baker B M.; Nerurkar N L, Burdick J A, Li W J, Tuan R S & Elliott D M, *Tissue Eng Part B Rev*, 15(2) (2009) 171.
44 Zhang Q, Wang L, Wei Z, Wang X, Long S & Yang J, *J Polym Sci B*, 50(2012) 1004.
45 Haider S, Al-Zeghayer Y, Ali F A A, Haider A, Mahmood A & Al-Masry W A, *J Polym Res*, 20(2013) 105.
46 Heidari I, Mashhadi M M & Faraji G, *Chem Phys Lett*, 590(2013) 231.
47 Wei X, Xia Z, Wong S C & Baji A, *Int Exp comput Biomech*, 1(2009) 45.
48 Huang W, Jiang L, Luo J, Chen Z, Ren L & Li C, *Mater Manuf Processes*, 31(12) (2016) 1603.
49 Zhu Z, Chen X, Du Z, Huang S, Peng D, Zheng J & Wang H, *Mater Manuf Processes*, 31(6) (2016) 707.